Supplemental Materials

Molecular Biology of the Cell

Kobayashi *et al*.

Supplemental material

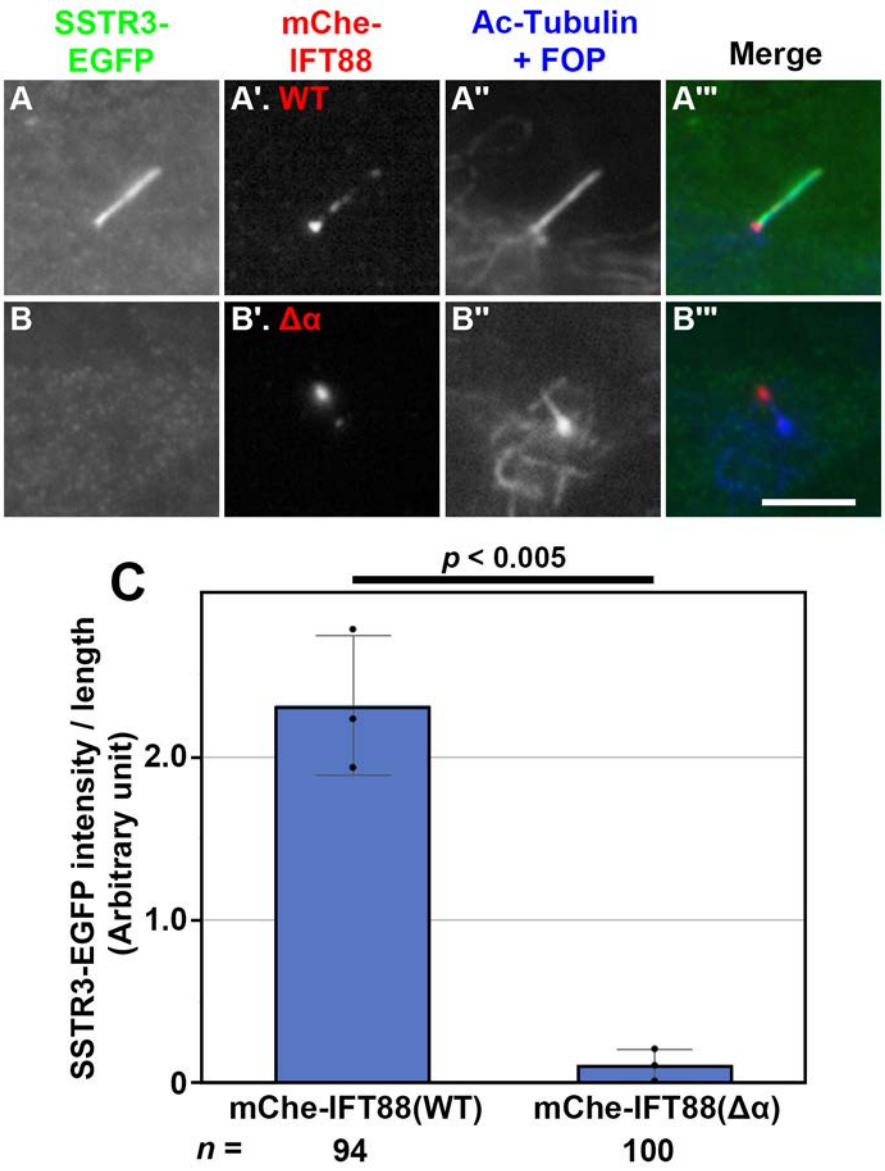

Fig. S1. A defect in the ciliary localization of SSTR3 in IFT88(Δα)-expressing *IFT88*-KO cells

SSTR3-EGFP was stably expressed in *IFT88*-KO cells stably expressing mChe-IFT88(WT) (A) or mChe-IFT88(Δα) (B), by infection of a lentiviral vector. The cells were then immunostained for mChe (A′, B′) and Ac-tubulin and FOP (A″, B″). Scale bar, 5 μm. (C) Ciliary SSTR3-EGFP intensities were measured, and the intensities per ciliary length are shown as a bar graph. Values are means ± SD of three independent experiments. In each set of experiments, 30 to 36 ciliated cells were observed, and the total number of ciliated cells observed (*n*) are shown. The *p*-value was determined by the Student *t*-test.

Table S1. Plasmid vectors used in this study

Vector	Insert	Reference
pTagRFP-T-N	Human IFT20	Katoh *et al.* (2016)
pTagRFP-T-C	Human IFT22	Katoh *et al.* (2016)
pTagRFP-T-C	Human IFT25	Katoh *et al.* (2016)
pTagRFP-T-C	Human IFT27	Katoh *et al.* (2016)
pTagRFP-T-C	Human IFT38	Katoh *et al.* (2016)
pCAG-EGFP-C	Human IFT46	Katoh *et al.* (2016)
pCAG-mCherry-C	Human IFT46	Katoh *et al.* (2016)
pCAG-EGFP-C	Human IFT52	Katoh *et al.* (2016)
pCAG-mCherry-C	Human IFT52	Katoh *et al.* (2016)
pTagRFP-T-C	Human IFT54	Katoh *et al.* (2016)
pCAG-mCherry-C	Human IFT56	Funabashi *et al.* (2017)
pTagRFP-T-C	Human IFT57	Katoh *et al.* (2016)
pCAG2-mCherry-C	Human IFT70A	Takei *et al.* (2018)
pCAG-EGFP-C	Human IFT70B	Katoh *et al.* (2016)
pCAG-mCherry-C	Human IFT70B	Katoh *et al.* (2016)
pCAG-mCherry-C	Human IFT74	Katoh *et al.* (2016)
pCAG2-mCherry-N	Human IFT80	This study
pCAG-mCherry-C	Human IFT81	Katoh *et al.* (2016)
pCAG2-EGFP-C	Human IFT88	This study
pCAG2-mCherry-C	Human IFT88	This study
pCAG2-EGFP-C	Human IFT88(ΔNT: 206–833)	This study
pCAG2-mCherry-C	Human IFT88(ΔNT: 206–833)	This study
pCAG2-EGFP-C	Human IFT88(ΔCT: 1–696)	This study
pCAG2-mCherry-C	Human IFT88(ΔCT: 1–696)	This study
pCAG2-EGFP-C	Human IFT88(Δα: 1–805)	This study
pCAG2-mCherry-C	Human IFT88(Δα: 1–805)	This study
pCAG-mCherry-C	Human IFT172	Katoh *et al.* (2016)
pEGFP-C1	Human IFT43	Hirano *et al.* (2017)
pmCherry-C1	Human IFT43	Hirano *et al.* (2017)
pCAG2-EGFP-C	Human IFT121	Hirano *et al.* (2017)

pCAG2-mCherry-C	Human IFT121	Hirano *et al.* (2017)
pCAG2-EGFP-C	Human IFT122	Hirano *et al.* (2017)
pCAG2-mCherry-C	Human IFT122	Hirano *et al.* (2017)
pCAG2-EGFP-C	Human IFT139	Hirano *et al.* (2017)
pCAG2-mCherry-C	Human IFT139	Hirano *et al.* (2017)
pCAG2-EGFP-C	Human IFT140	Hirano *et al.* (2017)
pCAG2-mCherry-C	Human IFT140	Hirano *et al.* (2017)
pCAG2-EGFP-C	Human IFT144	Hirano *et al.* (2017)
pCAG2-mCherry-C	Human IFT144	Hirano *et al.* (2017)
pEGFP-C1	Human TULP3	Hirano *et al.* (2017)
pCAG2-EGFP-C	Human KIF3A	Funabashi *et al.* (2018)
pCAG2-EGFP-C	Human KIF3B	Funabashi *et al.* (2018)
pCAG2-EGFP-C	Human KAP3	Funabashi *et al.* (2018)
pEGFP-C1	Human BBS2	Katoh *et al.* (2015)
pCAG-mCherry-C	Human BBS2	Nozaki *et al.* (2019)
pRRLsinPPT-EGFP-C	Human IFT88	This study
pRRLsinPPT-mCherry-C	Human IFT88	This study
pRRLsinPPT-mCherry-C	Human IFT88(ΔNT: 206–833)	This study
pRRLsinPPT-mCherry-C	Human IFT88(ΔCT: 1–696)	This study
pRRLsinPPT-EGFP-C	Human IFT88(Δα: 1–805)	This study
pRRLsinPPT-mCherry-C	Human IFT88(Δα: 1–805)	This study
pRRLsinPPT-EGFP-N	Mouse SSTR3	Hirano *et al.* (2017)
pGEX-6P1	GFP-nanobody	Katoh *et al.* (2015)

Video S1. TIRF microscopy of *IFT88*-KO cells expressing mChe-IFT88(WT)

Video S2. TIRF microscopy of control RPE1 cells expressing EGFP-IFT88(WT)

Video S3. TIRF microscopy of *IFT88*-KO cells expressing mChe-IFT88(Δα)

Video S4. TIRF microscopy of *IFT144*-KO cells expressing EGFP-IFT88(WT)

Video S5. ECV formation from *IFT88*-KO cells expressing EGFP-IFT88(Δα)

Supplemental references

Funabashi, T., Katoh, Y., Michisaka, S., Terada, M., Sugawa, M., and Nakayama, K. (2017). Ciliary entry of KIF17 is dependent on its binding to the IFT-B complex via IFT46-IFT56 as well as on its nuclear localization signal. Mol. Biol. Cell *28*, 624-633.

Funabashi, T., Katoh, Y., Okazaki, M., Sugawa, M., and Nakayama, K. (2018). Interaction of heterotrimeric kinesin-II with IFT-B-connecting tetramer is crucial for ciliogenesis. J. Cell Biol. *217*, 2867-2876.

Hirano, T., Katoh, Y., and Nakayama, K. (2017). Intraflagellar transport-A complex mediates ciliary entry as well as retrograde trafficking of ciliary G protein-coupled receptors. Mol. Biol. Cell *28*, 429-439.

Katoh, Y., Nozaki, S., Hartanto, D., Miyano, R., and Nakayama, K. (2015). Architectures of multisubunit complexes revealed by a visible immunoprecipitation assay using fluorescent fusion proteins. J. Cell Sci. *128*, 2351-2362.

Katoh, Y., Terada, M., Nishijima, Y., Takei, R., Nozaki, S., Hamada, H., and Nakayama, K. (2016). Overall architecture of the intraflagellar transport (IFT)-B complex containing Cluap1/IFT38 as an essential component of the IFT-B peripheral subcomplex. J. Biol. Chem. *291*, 10962-10975.

Nozaki, S., Castro Araya, R.F., Katoh, Y., and Nakayama, K. (2019). Requirement of IFT-B–BBSome complex interaction in export of GPR161 from cilia. Biol. Open *8*, bio043786.

Takei, R., Katoh, Y., and Nakayama, K. (2018). Robust interaction of IFT70 with IFT52–IFT88 in the IFT-B complex is required for ciliogenesis. Biol. Open *7*, bio033241.